Effect of Co^{2+}, Ni^{2+}, Cu^{2+}, or Zn^{2+} on Properties of Polyaniline Nanoparticles

Su Zhou, Tao Wu, Jinqing Kan

School of Chemistry and Chemical Engineering, Yangzhou University, Yangzhou 225002, People's Republic of China

ABSTRACT: Uniform polyaniline (PANI) nanoparticles with typical sizes of about 50 nm were electropolymerized on indium tin oxide surfaces in the presence of Co^{2+}, Ni^{2+}, Cu^{2+}, or Zn^{2+}. According to shaping theory, we first suggest the reason forming PANI spherical particles. Their conductivity, UV-vis spectra, FTIR spectra, X-ray diffraction, and thermogravimetric analysis were investigated. The conductivities and crystallinity of PANI doped with these ions are higher than those of PANI doped with HCl (PANI/HCl). Both UV-vis absorption spectra and FTIR spectra indicate the interactions between Co^{2+}, Ni^{2+}, Cu^{2+}, or Zn^{2+} and PANI chains. TG analysis also shows that the thermal stability of PANI doped by Co^{2+}, Ni^{2+}, Cu^{2+}, or Zn^{2+} is lower than that of PANI/HCl. © 2007 Wiley Periodicals, Inc. J Appl Polym Sci 106: 652–658, 2007

Key words: polyaniline; nanoparticles; SEM; FTIR; UV-vis

INTRODUCTION

Over the last years the trend toward miniaturization has led to the development of nanochemistry. Nanostructured (nanoparticles/rods/wires/fibers) conducting polymers having unusual physical and chemical properties have attracted great research interests. Much research has been conducted on the nanostructure of polyaniline (PANI) because it exhibits good environmental stability and its electrical properties can be modified by changing oxidation states and protonation states.[1,2] Nanostructures of PANI offer the possibility of enhanced performance since they combine the properties of low-dimensional organic conductors with high surface area materials. For example, in sensor applications, nanostructured PANI has greater sensitivity and swifter time response relative to its conventional bulk counterpart because of higher effective surface area and shorter penetration depth for target molecules.[3,4] Besides, PANI nanoparticles have been used in analytical separation,[5] proposed as diagnostics,[6] applied in electrorheological studies,[7] and catalysis.[8] Control of the particle morphology is desirable in various applications.[9,10]

Recently, various strategies including template synthesis, interfacial polymerization, self-assembly, and stepwise electrochemical deposition have been developed for the preparation of PANI nanostructures.[11–17] For example, PANI nanotubes or nanofibers with diameters <100 nm can be made by template-guided polymerization within channels of zeolites[18] or nanoporous membranes.[19–21] Adding structural directing molecules such as surfactants[22] or polyelectrolyte[23] to the chemical polymerization bath is another way to obtain PANI nanostructures. Electrospinning[24] can also produce conducting polymer nanofibers without templates. Many methods of preparing PANI nanostructures have been reported, but new simple and economical methods are still being explored.

Macromolecular complex forming interactions between PANI and metal ions give rise to novel chemical and physical properties.[25–33] However, it hardly reported effect of metal ions on morphology of PANI. In this article, we reported on a simple electrochemical method synthesized PANI nanoparticles through doping Co^{2+}, Ni^{2+}, Cu^{2+}, or Zn^{2+} during the polymerization and the effects of these ions on properties of PANI nanoparticle. The morphology of the PANI nanoparticle has been carefully analyzed using a scanning electron microscope (SEM) and transmission electron microscopy (TEM), and some characterizations of resulting products such as UV-vis spectroscopy, FTIR spectroscopy, conductivity, X-ray diffraction (XRD), and thermogravimetric analysis (TGA) are also shown.

EXPERIMENTAL

Chemicals

The monomer aniline (reagent grade) was distilled into colorless under reduced pressure prior to use.

Other chemicals were reagent grade and used as received without further treatment. All of the aqueous solutions were prepared with double distilled water.

Synthesis

The electrochemical polymerization of aniline was carried out in a classical one-compartment three-electrode cell at ambient temperature, approximately 20°C. An indium tin oxide conducting glass (ITO) or a platinum sheet was used as working electrode; another platinum sheet and a saturated calomel electrode (SCE) were used as counter electrode and the reference electrode, respectively. All potentials given here are referred to the SCE. PANI films were obtained using the method at 0.8 V in a solution containing 0.2 mol dm^{-3} aniline, 1.0 mol dm^{-3} hydrochloric acid (HCl), and 0.2 mol dm^{-3} $CoCl_2$, or 0.2 mol dm^{-3} $NiCl_2$, or 0.2 mol dm^{-3} $CuCl_2$ or 0.2 mol dm^{-3} $ZnCl_2$. Excellent cohesive films or product samples of PANI were formed on the ITO or platinum sheet. The films or product samples were rinsed with 1.0 mol dm^{-3} HCl. The product samples were dried at 78°C for 48 h.

Apparatus

A DH-1 potentiostat–galvanostat was used for electrochemical polymerization of aniline. The morphology and structures of resulting products were char-acterized by a scanning electron microscope (SEM XL-30 ESEM) and transmission electron microscope (TEM TENCNAI-12) and FTIR and UV-vis spectrometer, respectively. The UV-vis electronic absorption spectra of PANI films were obtained on a UV-2550 spectrometer (Shimadzu) in the range of 300–900 nm. Infrared (IR) spectra were recorded on an IFS66/S FTIR spectrometer (Bruker) at 4 cm^{-1} resolution on KBr pellets. TGA was performed using a STA 409PC instrument (NETZSCH), at a heating rate of 10°C min^{-1}, under nitrogen, from 30 to 700°C. Conductivity of the resulting products was measured using conventional four-probe technique on pressed pellets of the powder samples at 20°C. The thickness of the pellets for conductivity measurements is from 1.0 to1.5 mm. Wide-angle XRD patterns for the powder samples were taken on a M03XHF^{22} diffractometer (Mac Science, Japan), using Cu-Kα radiation (λ = 1.54056 Å), which was used to obtain the degree of crystallinity.

RESULTS AND DISCUSSION

The SEM morphology of the PANI films

Figure 1(a) shows the morphology of PANI film deposited onto ITO in solution containing 0.2 mol dm^{-3} aniline and 1.0 mol dm^{-3} HCl at 0.8 V for 15 min. It was seen from the SEM photographs that the diameters of PANI particles are larger than 200 nm, and the morphology of these particles is very irregular. When $CoCl_2$, $NiCl_2$, $CuCl_2$, or $ZnCl_2$ of same
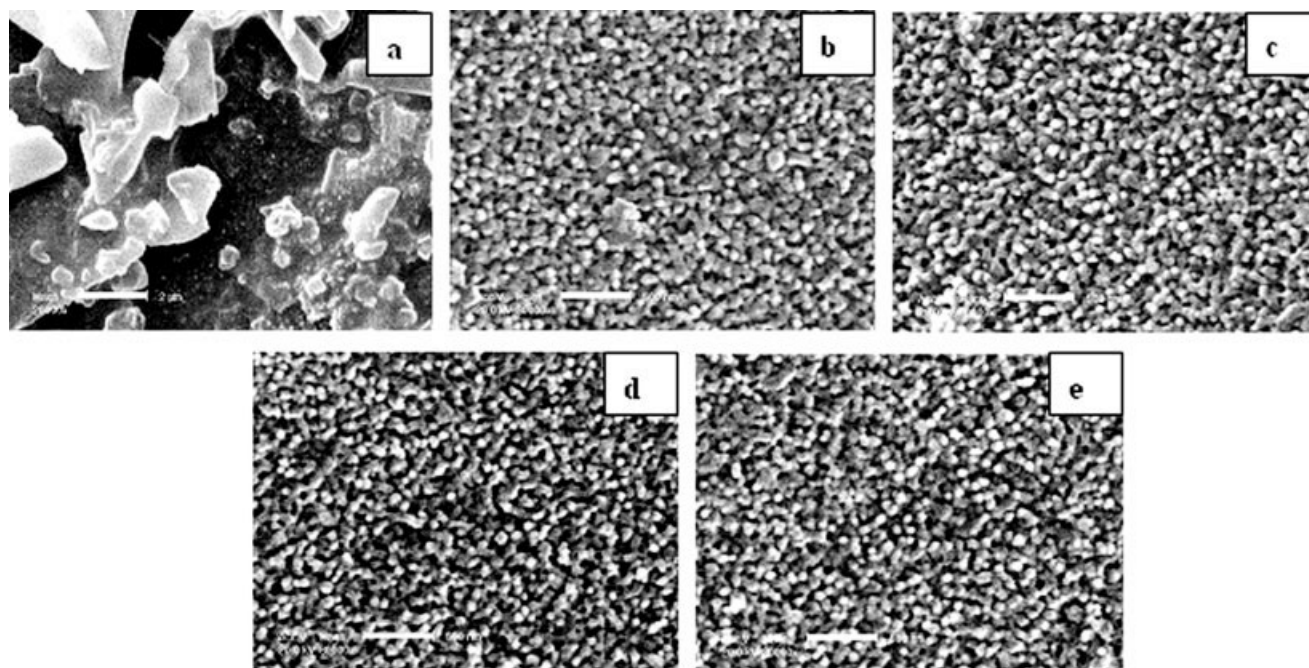

Figure 1 The morphology of PANI films electrochemical synthesized 15 min under different conditions: (a) HCl, (b) $CoCl_2$, (c) $NiCl_2$, (d) $CuCl_2$, and (e) $ZnCl_2$.
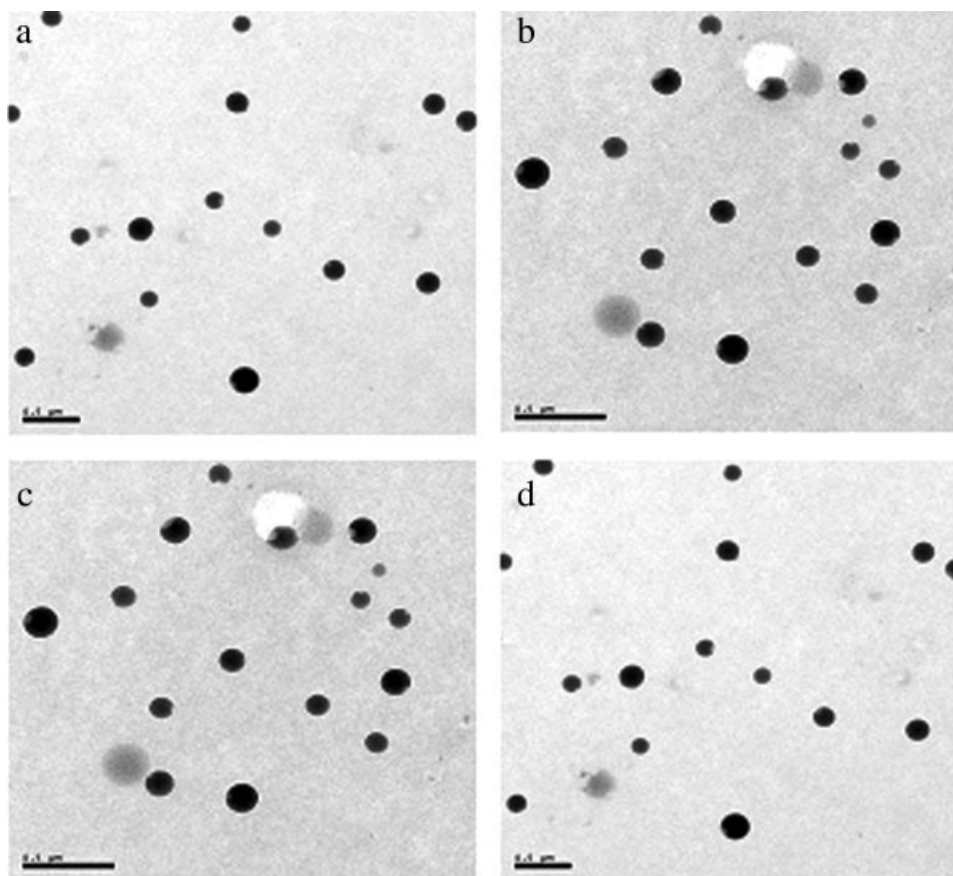
Figure 2 The TEM photographs of PANI electrochemical synthesized 15 min under different conditions: (a) $CoCl_2$, (b) $NiCl_2$, (c) $CuCl_2$, and (d) $ZnCl_2$.

molar ratio as aniline were added into the solution, the PANI film presents neat nanoparticles morphology [Fig. 1(b–e)] and the area fraction of nanoparticles with diameters of about 50–200 nm is over 95%. The results of TEM are consistent with those of SEM (Fig. 2). It has been reported that some cations can be doped inside PANI film and coordinate with PANI chains.[34] Because electron configurations of Co, Ni, Cu, or Zn are same as Fe, those ions may be similar to the interaction between Fe and N.[35] The lone-pair electrons of N atom in PANI chain interact with 3d orbit of Co, Ni, Cu or, Zn atom to form corn coordinate bond, which may lead to the alignment of PANI growth and form a more compact and uniform morphology. It is favorable for increase of electron transfer.[36]

Figure 3 is a schematic illustration formed spherical PANI particles. To understand the formation mechanism of PANI nanoparticles fully, we suggest that process is as follows: the PANI chains are firstly formed on ITO surface in the early stage of electropolymerization at constant potential. Then, Co^{2+}, Ni^{2+}, Cu^{2+}, or Zn^{2+} in the solution can coordinate with the lone-pair electrons of N atom in PANI chains. The coordination effect makes PANI chains

transform into the complex molecule with polar group [Fig. 3(a)]. The molecule is similar to surfactant. According to shaping theory, when the size of
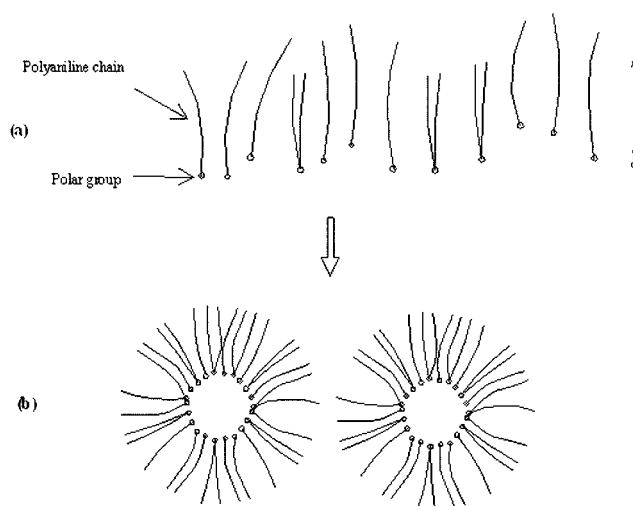

Figure 3 Schematic illustration of shaping process of spherical PANI particles. (a) The complex molecule with polar group; (b) the complex molecule aggregate into spherical particles.

TABLE I
The Effects of Different Transition-Metal Ions on Conductivity of Resulting Products

Sample	PANI-HCl	PANI/CoCl$_2$	PANI/NiCl$_2$	PANI/CuCl$_2$	PANI/ZnCl$_2$
κ/(S cm^{-1})	1.87	3.58	2.82	2.20	6.42

the molecule with polar group comes up to the proportion of the spherical particle morphology, it tends to aggregate spherical particles [Fig. 3(b)].[37] More studies are needed to be carried out to better understand the behavior of PANI aggregation in the presence of Co^{2+}, Ni^{2+}, Cu^{2+}, or Zn^{2+}.

Conductivity of resulting products

Table I gives the effects of Co^{2+}, Ni^{2+}, Cu^{2+}, or Zn^{2+} on the conductivity (κ) of the resulting products measured at 20°C. All samples were synthesized electrochemically in 1.0 mol dm^{-3} HCl aqueous solutions containing 0.2 mol dm^{-3} aniline with and without Co^{2+}, Ni^{2+}, Cu^{2+}, or Zn^{2+}. It can be seen clearly from Table I that compared with PANI/HCl, the conductivities of PANI doped with Co^{2+}, Ni^{2+}, Cu^{2+}, or Zn^{2+} are increased. Moreover, conductivity of PANI doped by Zn^{2+} and Co^{2+} are higher than that of PANI doped by Ni^{2+} and Cu^{2+}. The phenomenon was assigned to the interaction between Co^{2+}, Ni^{2+}, Cu^{2+}, or Zn^{2+} and PANI, which make PANI chains form more regularly, and electron transfer increase along the chains and results in an increase of conductivity. Besides, according to the literature,[38] the PANI subchains become more rigid and ordered under the influence of some metal ions, which leads to a high degree of crystallinity. It has been known[39,40] that PANI of higher crystallinity has a higher conductivity than that of amorphous PANI. Why are conductivities of PANI doped by Zn^{2+} and Co^{2+} higher than that of the others? This may be relevant to the radius of metal ions and the strength of coordination effect. It can be found from the result of experiment that the bigger the radius of metal cation is and the weaker the coordination effect between PANI and metal ions is, the higher the conductivity of PANI is.

UV-vis spectra of PANI

Figure 4 shows UV-vis absorption spectra of PANI films deposited onto ITO, which was obtained in solution containing 0.2 mol dm^{-3} aniline, 1.0 mol dm^{-3} HCl with and without Co^{2+}, Ni^{2+}, Cu^{2+}, or Zn^{2+}. The PANI films formed at different conditions [Fig. 4(a–e)] show three characteristic absorption bands at around 355, 440, and 845–860 nm. The characteristic peaks of PANI films appear at about 355 nm because of π-π* transition of the benzenoid ring and at about 440 nm and 845–860 nm because of polaron-π* and π-polaron band transitions,[41] respec-

tively. This shows that the above-mentioned PANI films are in the doped state.

Compared with the PANI films doped by only protonic acids [Fig. 4(a)], the absorption peaks [Fig. 4(b–e)] at 355nm due to π-π* transition of the benzenoid rings and about 440 nm due to the polaron-π* bands are almost not shifted, and the peaks due to π-polaron transition of PANI films obtained with Co^{2+}, Ni^{2+}, Cu^{2+}, or Zn^{2+} appear at the longer wavelength (from 845 to 855 nm, 860, 850, and 860 nm). The red shift implied that there exists interaction between metal ions and PANI chains,[42] which makes the energy gap of π-polaron narrower. Besides, it is seen from the red shift of UV-vis absorption spectra that the existence of metal ions can enhance the delocalized area of conjugated π-electron. This is consistent with the result of conductivity.

FTIR spectra of PANI

Figure 5 shows that the FTIR spectra of resulting products, which were synthesized electrochemically in the solution containing 0.2 mol dm^{-3} aniline, 1.0 mol dm^{-3} HCl with and without Co^{2+}, Ni^{2+}, Cu^{2+}, or Zn^{2+}. The bands assignments of Figure 4 are summarized in Table 2. The characteristic peaks at about 1574 and 1492 cm^{-1} are attributed to the stretching vibrations of N=Q=N ring, N—B—N ring, respectively. The peak at 1300 cm^{-1} corresponds to C—N
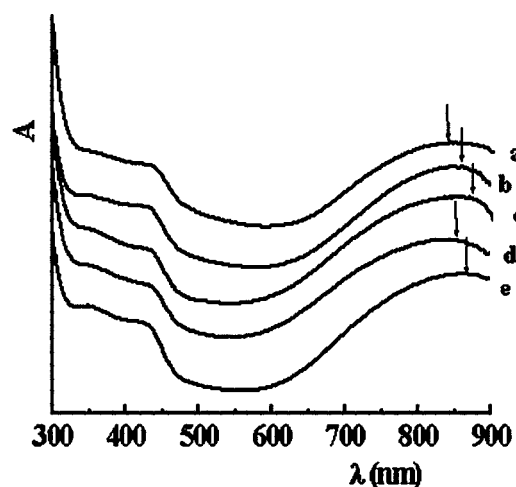

Figure 4 UV-vis absorption spectra of PANI films deposited onto the ITO at constant potential of 0.8 V, polymerization time is 15 min. (a) HCl, (b) NiCl$_2$, (c) CoCl$_2$, (d) CuCl$_2$, and (e) ZnCl$_2$.
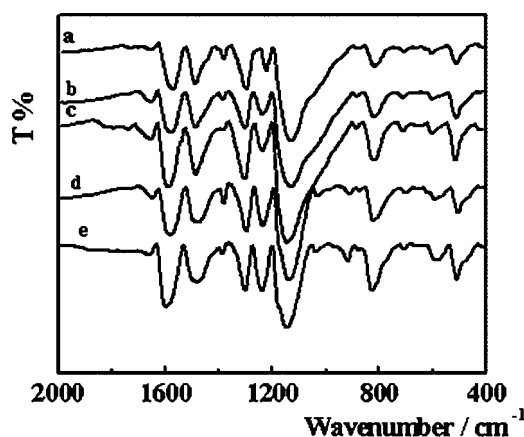
Figure 5 FTIR spectra of PANI electrochemical synthesized in different solutions at constant potential of 0.8 V. (a) HCl, (b) CoCl$_2$, (c) NiCl$_2$, (d) CuCl$_2$, and (e) ZnCl$_2$.

Figure 6 The XRD patterns of PANI electrochemical synthesized in different solutions at constant potential of 0.8 V. (a) HCl, (b) CoCl$_2$, (c) NiCl$_2$, (d) CuCl$_2$, and (e) ZnCl$_2$.

stretching vibration. The peaks at 1126 and 808 cm^{-1} are attributed to the characteristic of B—NH—Q or B—NH—B bonds, and out-of-plane bending vibration of C—H of benzene rings (where B refers to the benzenic-type rings and Q refers to the quinonic-type rings). The PANI spectra present a good agreement with the literature,[43,44] except for a few shifts in the wavenumbers. In addition, for all samples the bands located at about 3400 cm^{-1} and about 3200 cm^{-1} because of N—H bond stretching are not shown here.

When PANI were obtained in solution containing Co^{2+}, Ni^{2+}, Cu^{2+}, or Zn^{2+}, the peaks (curve b–d) of the quinoid unit shift to the higher wavenumber, other peaks are almost not shifted. Concretely, the existence of Co^{2+}, Ni^{2+}, Cu^{2+}, or Zn^{2+} makes the peak of the stretching vibrations of N=Q=N ring shift from 1574 to 1582 cm^{-1}, 1593, 1593, and 1600 cm^{-1}, respectively. In addition, the characteristic of B—NH—Q or B—NH—B bonds shifts 6–20 cm^{-1} towards higher wavenumber when doping with those ions. According to the precision of TENSOR 27 FTIR spectrometer (4 cm^{-1}), the peaks shift of FTIR spectra may be caused by the coordination interaction between PANI chains and metal ions. It is in agreement with the conclusions of UV-vis spectra. Besides, compared with PANI doped by different metal ions, the peaks of the quinoid unit of PANI
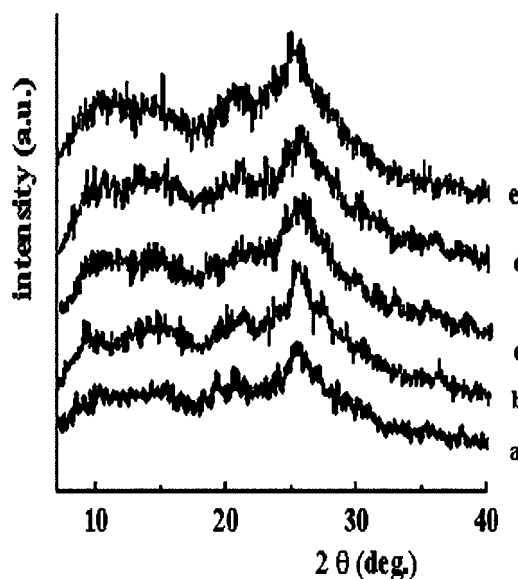
doped by Zn^{2+} have much greater shifts. The reason is not clear yet.

X-ray diffraction spectra

Figure 6 shows the XRD patterns of the PANI prepared in the solution containing 0.2 mol dm^{-3} aniline, 1.0 mol dm^{-3} hydrochloric acid with and without Co^{2+}, Ni^{2+}, Cu^{2+}, or Zn^{2+}. The XRD profiles of the PANI with metal ions are similar to that of the PANI without metal ions. However, the degree of crystallinity of PANI doped with transition metal ions is larger than that of PANI/HCl. There are several diffraction peaks between 2θ-values of 8 and 30°in the samples, which reveal the local crystallinity of PANI.[45–47] The peak of 2θ = ∼ 9° was assigned as the scattering along the orientation parallel to the PANI chain,[48] and the bands at approximately 2θ-values of 15 and 22° demonstrated a partially amorphous nature.[49] The peaks at 2θ = ∼ 25° may be caused by the periodicity perpendicular to the polymer chain.[49] These results indicate that the PANI chains become more ordered under the influence of

TABLE II
FTIR Band Assignments of Samples in Figure 5

Sample	C=C quinoid ring (cm^{-1})	C=C benzoid ring (cm^{-1})	C—N (cm^{-1})	C=C quinoid ring (cm^{-1})	C—H (cm^{-1})
a	1574	1492	1300	1126	815
b	1582	1490	1305	1132	820
c	1593	1489	1305	1144	815
d	1593	1487	1304	1146	820
e	1600	1487	1300	1146	820

metal ions, the degree of crystallinity is higher for PANI doped with metal ions than that of PANI/HCl.

This higher crystallographic order of PANI chains causes a decreased separation of the chains and increased conductivity. It has been reported that PANI of higher crystallinity has a higher conductivity than amorphous one,[39] so it was understandable that the conductivity of PANI doped with Co^{2+}, Ni^{2+}, Cu^{2+}, or Zn^{2+} is higher than that of PANI/HCl.

TG analysis

Figure 7 shows that the TG curves of resulting products, which were prepared in solution containing 0.2 mol dm^{-3} aniline, 1.0 mol dm^{-3} HCl with and without Co^{2+}, Ni^{2+}, Cu^{2+}, or Zn^{2+}, the temperature range taken between 30 and 700°C. From the TG curves, we can see clearly that the weight looses of PANI samples (curve b–d) in different temperature ranges. All samples shown in Figure 6 exhibited a similar thermal behavior, with a small variation in degradation temperature. In general, the thermal behavior of the PANI/HCl shows a three-step weight loss process, the first stage weight loss from 50 to 140°C is about 7%, which was attributed to the loss of water entrapped in the PANI and low molecular weight oligomers.[50,51] The second weight loss ranging from 150 to 300°C is believed to be due to the elimination of acid dopant (HCl)[52–54] and the third weight loss starting at about 350°C corresponds to thermal decomposition of PANI backbone chains.[55,56]

As for the PANI prepared with Co^{2+}, Ni^{2+}, Cu^{2+}, or Zn^{2+}, the thermal decomposition temperature of PANI with metal ions is lower than that of PANI without metal ions by about 50°C, which implies the thermal stability of PANI prepared with Co^{2+}, Ni^{2+},
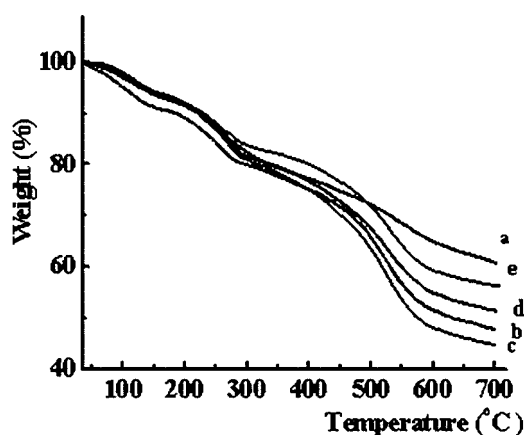
Cu^{2+} or Zn^{2+}, decreases. It is probably due to that those ions can interact with PANI chains, and result in the decrease of the PANI thermal stability.[57]

CONCLUSION

In summary, a facile and economical electrochemical method to synthesize the nanoparticles of PANI with Co^{2+}, Ni^{2+}, Cu^{2+}, or Zn^{2+} was introduced. The SEM photographs show that PANI nanoparticles with typical size of about 50nm can be prepared on ITO in the presence of Co^{2+}, Ni^{2+}, Cu^{2+}, or Zn^{2+}. Both UV-vis absorption spectra and FTIR spectra indicate the interactions between these ions and PANI chains. The conductivities and crystallinity of PANI doped with these ions are higher than those of PANI/HCl. TG analysis also shows that the thermal stability of PANI doped with Co^{2+}, Ni^{2+}, Cu^{2+}, or Zn^{2+} is lower than that of PANI/HCl.

Figure 7 The TG analysis of PANI electrochemical synthesized in different solutions at constant potential of 0.8 V. (a) HCl, (b) $CoCl_2$, (c) $NiCl_2$, (d) $CuCl_2$, and (e) $ZnCl_2$.

References

1. Palaniappan, S. Euro Polym J 2001, 37, 975.
2. Moraes, S. R.; Huerta-Vilca, D.; Motheo, A. J. Euro Polym J 2004, 40, 2033.
3. Huang, J.; Virji, S.; Weiller, B. H.; Kaner, R. B. J Am Chem Soc 2003, 125, 314.
4. Liu, J.; Lin, Y.; Liang, L.; Voigt, J. A.; Huber, D. L.; Tian, Z. R.; Coker, E.; Mckenzie, B.; Mcdermott, M. J. Chem Eur J 2003, 9, 605.
5. Nagaoka, T.; Nakao, H.; Suyama, T.; Ogura, K.; Oyama, M.; Okazaki, S. Anal Chem 1997, 69, 1030.
6. Goller, M. I.; Barther, C.; McCarthy, G. P.; Corradi, R.; Newby, B. P.; Wilson, S. A.; Armes, A. P.; Luk, S. Y. Colloid Polym Sci 1998, 276, 1010.
7. Kuamoto, N.; Takahashi, Y.; Nagai, K.; Koyama, K. React Funct Polym 1996, 30, 367.
8. Huang, S. W.; Neoh, K. G.; Kang, E. T.; Han, H. S.; Tan, K. L. J Mater Chem 1998, 8, 1743.
9. Stejskal, J.; Kratochvil, P.; Gospodinova, N.; Terlemezyan, L.; Mokreva, P. Polymer 1992, 33, 4857.
10. Stejskal, J.; Spirkova, M.; Riede, A.; Helmstedt, M.; Morkreva, P.; Prokes, J. Polymer 1999, 40, 2487.
11. Huang, J.; Virji, S.; Weiller, B. H.; Kaner, R. B. Chem Eur J 2004, 10, 1314.
12. Huang, J.; Kaner, R. B. Angew Chem Int Ed 2004, 43, 5817.
13. Dong, H.; Prasad, S.; Nyame, V.; Jone, W. E. Chem Mater 2004, 16, 371.
14. Carswell, A. D. W.; Rear, E. A. O.; Grady, B. P. J Am Chem Soc 2003, 125, 14793.
15. Kim, D.; Choi, J.; Kim, J. Y.; Han, Y. K.; Sohn, D. Macromolecules 2002, 13, 5314.
16. Ma, Y.; Zhang, J.; Zhang, G.; He, H. J Am Chem Soc 2004, 126, 7097.
17. Huang, J.; Kaner, R. B. J Am Chem Soc 2004, 126, 851.
18. Wu, C. G.; Bein, T. Science 1994, 266, 1013.
19. Martin, C. R. Acc Chem Res 1995, 28, 61.
20. Wang, C. W.; Wang, Z.; Li, M. K.; Li, H. L. Chem Phys Lett 2001, 341, 431.
21. Wang, Z.; Chen, M. A.; Li, H. L. Mater Sci Eng A 2002, 328, 33.
22. Yu, L.; Lee, J. I.; Shin, K. W.; Park, C. E.; Holze, R. J Appl Polym Sci 2003, 88, 1550.

23. Liu, J. M.; Yang, S. C. J Chem Soc Chem Commun 1991, 21, 1529.
24. MacDiarmid, A. G.; Jones, W. E.; Norris, I. D.; Gao, J.; Johnson, A. T.; Pinto, N. J.; Hone, J.; Han, B.; Ko, F. K.; Okuzaki, H.; Llaguno, M. Synth Met 2001, 119, 27.
25. Lipovski, A. A.; Kolobkova, E. V.; Olkhovets, A.; Petrikov, V. D.; Wise, F. Physica E 1999, 5, 157.
26. Godovsky, D. Y.; Varfolomeev, A. E.; Zaretsky, D. F.; Nayana Chandrakanthi, R. L.; Kundig, A.; Weder, C. J Mater Chem 2001, 11, 2465.
27. Shipley, C. P.; Capecchi, S.; Salata, O. V.; Etchells, M.; Dobson, P. J.; Christou, V. Adv Mater 1999, 11, 533.
28. Lin, Q.; Shi, C. Y.; Liang, Y. J.; Zheng, Y. X.; Wang, S. B.; Zhang, H. J. Synth Met 2000, 114, 373.
29. Kobayashi, N.; Uemura, S.; Kusabuka, K.; Nakahira, T.; Takahashi, H. J. Mater Chem 2001, 11, 1766.
30. Wu, C. G.; Hsiao, H. T.; Yeh, Y. R. J Mater Chem 2001, 458, 2287.
31. Cazeca, M. J.; Chittibabu, K. G.; Kim, J.; Kumar, J.; Jain, A.; Kim, W. Synth Met 1998, 98, 45.
32. Male, N. A. H.; Salata, O. V.; Christou, V. Synth Met 2002, 126, 7.
33. Turro, N. J.; Chow, M. F.; Chung, C. J.; Weed, G. C.; Kraeutler, B. J Am Chem Soc 1980, 469, 4843.
34. Forsberg, J. H. Coordination Chem Rev 1973, 10, 195.
35. Deng, J. G.; He, C. L.; Long, X. P.; Peng, Y. X.; Li, P.; Chen, X. Z.; Yu, G. C. Gaofenzi Cailiao Kexue 2004, 20, 149.
36. Cai, L. T.; Yao, S. B.; Zhou, S. M. Synth Met 1997, 88, 205.
37. Hartel, S.; Fanani, M. L.; Maggio, B. Biophys J 2005, 88, 287.
38. Lv, R. G.; Tang, R.; Kan, J. Q. Mater Chem Phys 2006, 95, 294.
39. Kim, B. J.; Oh, S. G.; Han, M. G.; Im, S. S. Synth Met 2001, 122, 297.
40. Lu, F. L.; Wudll, F.; Nowak, M.; Heeger, A. J. J Am Chem Soc 1986, 108, 8311.
41. Stafstrom, S.; Breadas, J. L.; Epstein, A. J.; Woo, H. S.; Tenner, D. B.; Huang, W. S.; Macdiarmid, A. G. Phys Rev Lett 1987, 59, 1464.
42. Zeng, X.; Ko, T. J Polym Sci Part B: Polym Phys 1997, 35, 1993.
43. Laska, J.; Widlarz, J. Polymer 2005, 46, 1485.
44. Cheng, D. M.; Ng, S.-C.; Chan, H. S. O. Thin Solid Films 2005, 477, 19.
45. Svetlicic, V.; Schmidt, A. J.; Miller, L. L. Chem Mater 1998, 10, 3305.
46. Joo, J.; Chung, Y. C.; Song, H. G.; Baeck, J. S.; Lee, W. P.; Epstein, A. J.; MacDiarmid, A. G. Synth Met 1997, 84, 739.
47. Pouget, J. P.; Jozefowicz, M. E.; Epstein, A. J.; Tang, X.; MacDiarmid. A. G. Macromolecules 1991, 24, 779.
48. Moon, Y. B.; Cao, Y.; Smith, P.; Heeger, A. J. Polym Commun 1989, 30, 196.
49. Trivedi, D. C.; Dhawan, S. K. Synth Met 1993, 58, 309.
50. Chan, H. S. O.; Ho, P. K. H.; Khor, E.; TanK, M. M.; Tan, L.; Tan, B. T. G.; Lim, Y. K. Synth Met 1989, 31, 95.
51. Palaniappan, S.; Narayana, B. H. J Polym Sci Part A: Polym Chem 1994, 32, 2431.
52. Campos, T. L. A.; Kersting, D. F.; Ferreira, C. A. Surf Coat Technol 1999, 122, 3.
53. Chan, H. S. O.; Teo, M. T. B.; Khor, E.; Lim, C. N. J Thermal Anal 1989, 35, 765.
54. Neoh, K. G.; Kang, E. T.; Tan, K. L. Thermochim Acta 1990, 171, 279.
55. Oh, S. Y.; Kop, H. C.; Choi, J. W.; Rhee, H. W.; Kim, H. S. Polymer J 1997, 29, 404.
56. Wei, Y.; Hsueh, K. F. J Polym Sci Part A: Polym Chem 1989, 27, 4351.
57. Pielichowski, K. Solid State Ionics 1997, 104, 123.